

Synthesis Of Polymer Capped Ag, Cu And Ni Nanoparticles And Kinetic Studies On The Photocatalytic Degradation Of Pharmaceutical Pollutants

Santhanamari Thiyagarajan^{1*} and Subramanian Kanchana²

¹*Department of Medical Laboratory Technology, Faculty of Applied Medical Sciences, Northern Border University, Arar-91431, Saudi Arabia*

²*Department of Chemistry, Quaid-E-Millath Government College for Women (Autonomous), Chennai-600002, India*

**Author for Correspondence:*

Dr. Santhanamari Thiyagarajan,

Department of Medical Laboratory Technology,

Faculty of Applied Medical Sciences, Northern Border University, Arar, Kingdom of Saudi Arabia, P.O. Box: 01321; Zip code: 91431,

E-mail: drsthiyagarajan@live.com, Thiyagarajan.S@nbu.edu.sa

ORCID iD: 0000-0001-7943-8707

This study investigated the catalytic efficiency of two groups of Ag, Cu and Ni metal nanoparticles, each prepared in PEG and PVP polymers, for the degradation of three common pharmaceutical pollutants of the natural aquatic bodies. Chemical synthesis by means of reduction of metal salts resulted in the production of nanoparticles ranging in sizes of 12 ± 1 to 22 ± 1 nm. Therapeutic drugs Polybion (PB), Neurobion Forte (NB) and Methycobal (MC) were subjected to photocatalytic reduction in the presence of NaBH_4 reductant independently under solar and UV irradiations at 25°C . Experimental photocatalysis was carried out in a one pot batch reactor and the kinetics of degradation of drugs were recorded in terms of irradiation time vs. absorbance linear relationships. The pseudo first order rate coefficient values indicated the constant λ_{max} equal to 216 nm, 275 nm and 230 nm corresponding to PB, NB and MC respectively. The trend of drug degradation of the drugs based on the catalytic efficiency (ϕ_c) and rate coefficient (k) values of nanoparticles was $\text{Cu} > \text{Ag} > \text{Ni}$. A constant catalyst loading of 5mg for 20ml of 1mM of drug solution along with 1ml of 5% by weight of NaBH_4 in aqueous solution demonstrated the trend of photocatalytic degradation rate constants in the order of $\text{MC} > \text{NB} > \text{PB}$. Keeping all the conditions of the experiment constant, the catalytic efficiencies of metal nanoparticles were better augmented by the PEG stabilizer and the solar radiation than their counterparts.

INTRODUCTION

Steadily increasing population, indiscriminate industrialization and growing urbanization worldwide are attributed to the irreversible environmental damage. Discharge of effluents

along with the byproduct chemicals, dyes, pesticides, pharmaceuticals, etc. by the manufacturing industries contribute organic pollutants to the terrestrial environment and natural aquatic bodies such as rivers, lakes, ponds and so on.

Pharmaceutical drugs such as Polybion (PB), Neurobion (NB) and Methycobal (MC) are found in the environmental water resources due to their wide spread and intense applications [1]. These drugs fall under the important group of vitamin supplements used in the treatment of human and veterinary deficiencies [2]. Due to the prolonged discharge in the environment, these substances have infused into soil, ground water and river sources etc. in alarmingly high concentrations [3, 4]. The MC is an extensively used pro-antibiotic and have been detected in high concentrations in drinking water, river resources etc. The MC contaminated water have exhibited high stability towards conventional biodegradation and chlorination methods. The NB belong to the most important class of synthetic antibiotics used in supplements for human and veterinary medicines. Since the NB possess polar structure, it is not significantly absorbed in the subsoil and gets leached significantly into the water resources.

Considerable attention has been paid in recent years in exploring various methods for the degradation for these three drugs PB, NB and MC. Conventional methods of wastewater treatment such as electrochemical methods, adsorption, ultrafiltration, activated carbon, etc. are time consuming and expensive and less efficient [5]. The heterogeneous photocatalysis is considered as an effective and eco-friendly method for the remediation of polluted water. This method causes complete degradation of organic pollutants with the use of natural energy source and does not cause the formation of polycyclic products or toxic products [6-8]. Photocatalytic degradation of organic pollutants is carried out through using semiconductor catalysts and common light energy sources such as UV, solar radiation and visible light [9, 10].

The emergence of metal nanoparticles (M-nps) possessing enhanced catalytic properties for advanced oxidation processes has facilitated the efficient treatment of waste water containing pharmaceutical pollutants in recent years. The M-nps, once activated by sunlight in aqueous solutions, serve as sensitizers to enhance the photodecomposition of organic pollutants by way of a light-induced redox mechanism [7, 11]. Synthesis of transition M-nps capped with synthetic stabilizers such as poly N-vinyl pyrrolidone and utilizing them for the cost-effective treatment of industrial effluents containing chemical and bio-medical wastes has drawn remarkable attention among the researchers [12].

Previous research studies focusing on the remediation of pharmaceutical pollutants have explored the catalytic properties of metal oxide nanoparticles or nanocomposites for the photocatalytic degradation processes. Literatures concerning the utilization of transition metal nanoparticles for the chemical reduction of pharmaceutical drugs is scarce. Nanoparticles of transition metals like Ag, Cu and Ni can be considered as as better catalysts due to their low cost, abundant availability and stability. Therefore, the present study was carried out to explore the nanoparticles of Ag, Cu and Ni for their heterogeneous catalytic potential in the photo degradation of three dugs in aqueous medium and to suggest them for application in the remediation of pharmaceutical pollutants in natural environment.

MATERIALS AND METHODS

Synthesis of Metal nanoparticles

The synthesis of M-nps was performed using a modified wet chemical reduction method [13]. For the chemical synthesis of nanoparticles of silver, copper and nickel and metals reduction of silver nitrate (AgNO_3), copper chloride ($\text{CuCl}_2 \cdot 2\text{H}_2\text{O}$) and nickel chloride ($\text{NiCl}_2 \cdot 6\text{H}_2\text{O}$) along with hydrazine hydrate ($\text{N}_2\text{H}_4 \cdot \text{H}_2\text{O}$) in the presence of stabilizing agents such as PEG (biopolymer) and PVP (synthetic polymer) was carried out. Ideally, the raw materials of these metals (0.350 g) along with the polymeric stabilizer (0.25 g) were subjected to ultrasonic dispersion in anhydrous ethanol (50 mL) and EG (50 mL) mixture for 30 – 40 min. The pH of the mixture was adjusted to 12.0 using NaOH (0.1 M) and heated to 70°C. Then, hydrazine hydrate ($\text{N}_2\text{H}_4 \cdot \text{H}_2\text{O}$) anhydrous ethanol (10 mL) was added dropwise to the reaction solution and left for 4 hours at 80°C along with intermittent stirring. The resultant of the reaction containing M-nps was brought to the room temperature. The M-nps in anhydrous ethanol solution were centrifuged, washed and air dried for future use.

Characterization of Metal nanoparticles

The synthesized M-nps were characterized using the techniques such as UV–visible spectrophotometry, X-ray diffraction analysis, FTIR, electron microscopy and EDX spectroscopy. UV–visible spectra analysis in terms of absorption maxima was carried out at wavelengths of 200–700 nm. The FTIR examination was performed to detect the biomolecules that contribute for efficient stabilization of M-nps. The size, crystalline shape and distribution of M-nps were evaluated by X-ray diffraction method (XRD), high resolution transmission electron microscopy (HR-TEM) and dynamic light scattering (DLS) analysis respectively. The scanning electron microscopy coupled with built-in 200 kV field-emission (FE-SEM) gun operating at room temperature ($25 \pm 1^\circ\text{C}$) was utilized for the detailed study on the morphology of M-nps. Analysis of elemental composition of M-nps was performed by using energy-dispersive X-ray (EDX) spectroscopy.

Catalytic degradation of Pharmaceutical drugs

One pot batch reactor with pseudo first order conditions was utilized for carrying out the reductive degradation of selected drugs. Stock solutions (1mM; pH 7.0) of the drugs PB, NB and MC were prepared in deionized distilled water. A 100 mL glass double walled three necked round bottomed flask fitted with magnetic stirrer served as the reactor. In each experiment, 20 mL of drug solution was taken to which 0.5 mg of nano catalyst was added. The solution was mixed with aqueous 5% NaBH_4 (wt/v) solution. In order to provide the artificial light source of UV light irradiation to the reaction mixture, a mercury lamp (120 W) was mounted on the top of the reactor. By means of circulating H_2O into the double walled assembly, a constant temperature of 25°C was maintained and the reduction reaction was carried out for three days. The reaction mixture was subjected to vigorous stirring throughout the process. Monitoring of reduction reaction was performed using a UV-vis spectrophotometer. The absorbance at 275 nm for NB, 230 nm for MC and 216 nm for PB were used to calculate the equilibrium adsorption of the drugs.

Aliquots of drug solution (0.5mL) from the reaction mixture were drawn out at regular time intervals for assessment of parameters controlling the trend of reductive degradation of each drug system. For each of processes carried out under solar and UV irradiations, separate kinetic parameters were determined. Kinetic study was performed by measuring the wavelengths at maximum and low absorbance values for each of the drug. By way of recording the absorbance variations with time i.e., 50% decomposition the rate constants of the drug degradations were determined. Pseudo first order conditions were ensured by using ten times higher concentration of the reductant (NaBH_4) than that of the drug. Linear kinetic plots were generated through calculating the values by multiplying them with that of the constant (2.303). Determination of the pseudo first order rate coefficient values from the kinetic plots was done by plotting $\log(\text{OD}_0/\text{OD}_t)$ versus time. Catalytic efficiency (ϕ_c) of M-nps for the reductive degradation reaction was determined as follows:

$$\phi_c = k_c/k_0,$$

Where, rate constants k_c (presence) and k_0 (absence) of catalysts.

For the purpose of studying the effects of polymeric biostabilizer (PEG) and the synthetic stabilizer (PVP) on the catalytic properties of Ag, Cu and Ni nps catalyst systems, the rate coefficient values of the degradation of each of the drug system at constant pH were determined.

RESULTS AND DISCUSSION

Characterization of M-nps

From the UV–Vis spectra, the maximum absorbance of Ag, Cu, Ni and nanoparticles were recorded at 410, 380 and 470 nm respectively (Fig. 1-3). The formation of M-nps was confirmed based on the appearance of respective peaks reflecting surface plasmon resonance (SPR) bands during the reaction [14]. The formation of SPR is attributed to the particle size, shape, interaction with the medium and the exchange of charge between the particle and the medium [15].

The FTIR spectra (Fig. 1-3) showed intense bands corresponding to H-bonded O-H stretch at 2832, 1583 and 3247 cm^{-1} respectively for Ag, Cu and Ni-nps. Bands indicating C-O stretch were recorded at 2941, 1892 and 3558 cm^{-1} for respective M-nps. Occurrences of C-F strong stretch for each of the M-nps indicated the formation of bands at 1244, 1275 and 1573 cm^{-1} . Muthukrishnan et al. [15] had reported similar values from their studies on M-nps. The analysis IR spectrum and the broad SPR bands deciphered the occurrences of different functionalities in the basic system of the biomolecules [16]. Analysis of X-ray diffraction of M-nps confirmed their pure phase and crystalline nature (Fig. 1-3). The 2θ values of diffraction peaks 32 to 77° corresponding to the lattice planes (125) to (438) were observed for the M-nps under study.

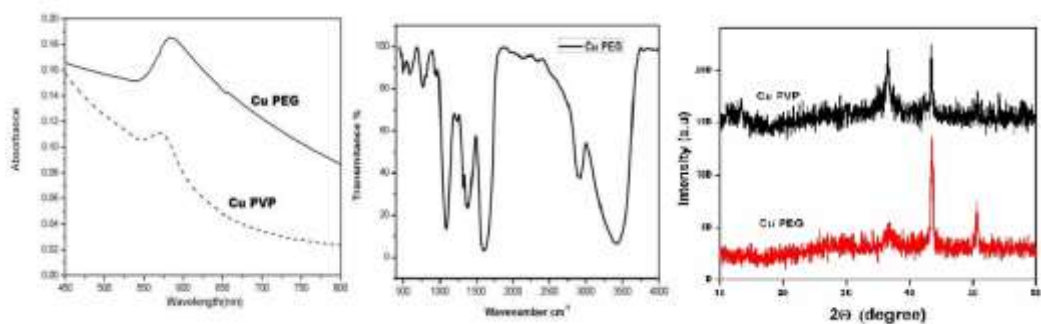


Fig. 1- UV-Vis Spectra, FTIR and XRD of Cu nanoparticles

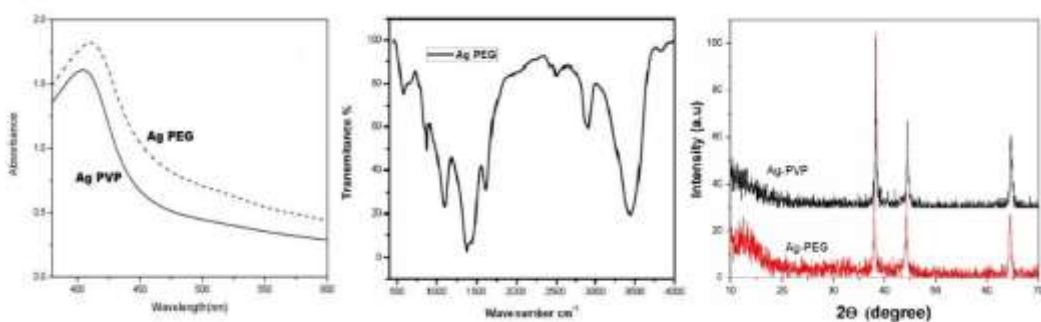


Fig. 2- UV-Vis Spectra, FTIR and XRD of Ag nanoparticles

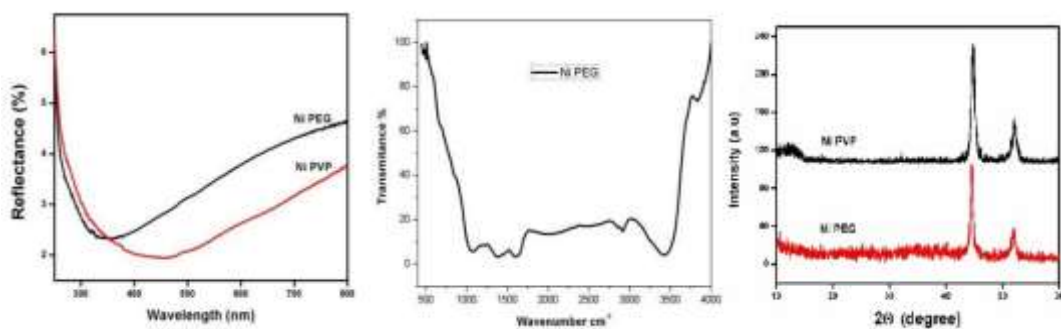


Fig. 3- UV-Vis Spectra, FTIR and XRD of Ni nanoparticles

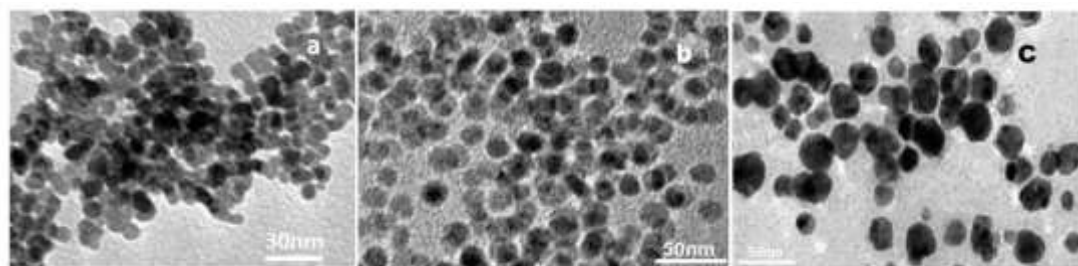


Fig. 4- TEM Micrographs of Cu (a), Ag (b) and Ni (c) nanoparticles

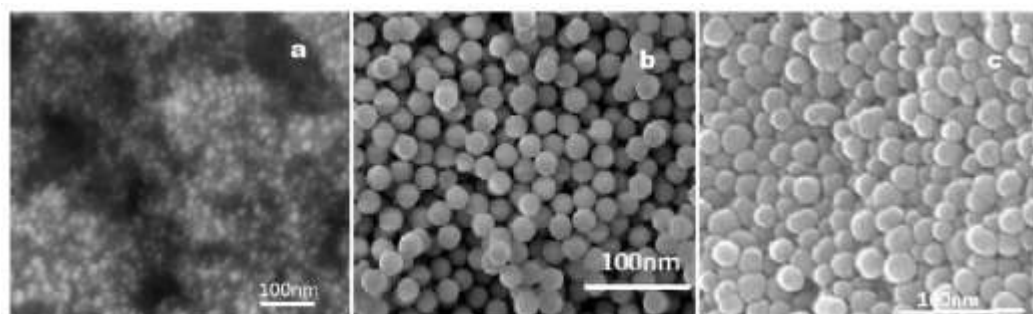


Fig. 5- FE-SEM Micrographs of Cu (a), Ag (b) and Ni (c) nanoparticles

The study of TEM micrographs indicated the morphological features of the M-nps. The particles of Ag and Cu were spherical to cubic and uniform in morphology and the Ni-nps appeared polycrystalline (Fig. 4). In general, the particles were discrete and non-agglomerated. Our observation is in agreement with the studies of Mntungwa et al. [17] and Basu et al. [18]. The average particle sizes calculated for PEG capped Ag, Cu and Ni-nps were 15 ± 1 nm, 12 ± 1 nm and 18 ± 1 nm, and, while for those PVP stabilized were 20 ± 1 nm, 15 ± 1 nm and 22 ± 1 nm respectively. The FE-SEM studies depicted distinct shapes of M-nps which remained un-agglomerated (Fig. 5). The EDX spectrum analysis for the detection of C, H, O and Ni elements corresponded the energy bands centered at 7.3, 3.7 and 8.2 keV respectively for Ag, Cu and Ni-nps indicating proper synthesis of M-nps [19].

Photo catalytic degradation experiment

The drug solutions when mixed with NaBH_4 (2% wt/v) and kept for more than 24 hours, degradative reduction occurred to the extent of only $<5\%$ as indicated by the colour intensity. In contrast, upon addition of M-nps to the NaBH_4 mixed dye solutions, within four hours of time, complete degradation of the drug was achieved. Despite the NaBH_4 serving as a reductant [20,21], the photo energy is a critical factor for of degradation of drug polluted effluents in the natural environment [22].

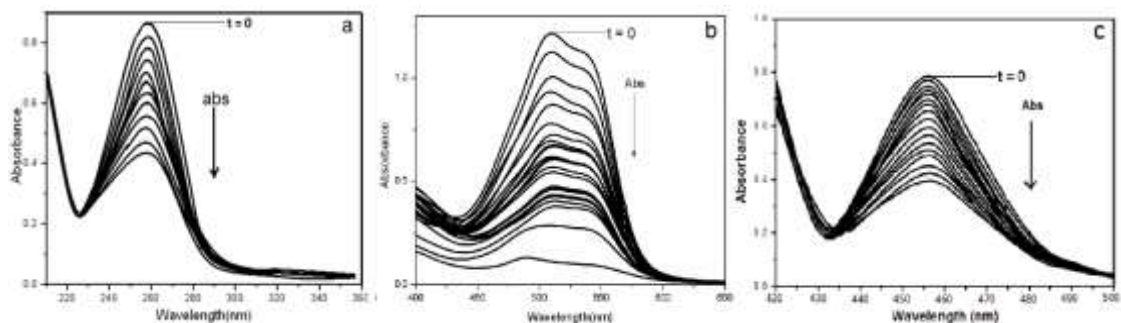


Fig. 6 - UV VIS spectra of Typical curves and Stacked curves of variation with time for reduced drugs a) Polybion b) Neurobion and c) Methycobal

The UV vis spectra of the treated drugs (Fig. 6) showed diminishing absorbance maxima (λ_{max}) of the dye solutions post the treatment process. The relative absorbance bands (λ_{max}) for PB, NB and MC in samples were observed at 216, 275 and 230 nm and respectively. The absorbance values gradually decreased after 30 min of the addition of Ag, Cu and Ni-nps to the drug. It was also noted that there was a balanced increase of SPR of M-nps. The time of contact of catalysts with the drug solution is a critical factor for photocatalysis in the treatment of polluted water. Proportionate with the contact time, the exposure of reactive sites nanocatalysts increases which helps in faster degradation of drugs [23].

Degradation kinetic studies

Degradation pattern of the three drugs represented by UV-Vis spectra are shown in figure 6. For the purpose of better understanding the catalytic process carried out by the M-nps, our study explains the absorbance versus time kinetics of photocatalytic degradation of three drugs in terms of the reaction catalyzed by Cu-nps for. Figures 7 and 8 depict the absorbance versus time variance plots for the catalysis of PEG and PVP stabilized Ag, Cu, and Ni-nps for the degradation of three drug systems. The absorbance maxima (λ_{max}) of the drugs diminished with time as the reaction proceeded. A recent work by Shetty et al. [24] on the photocatalytic degradation of pharmaceutical pollutants using N-doped TiO₂ reported similar observation.

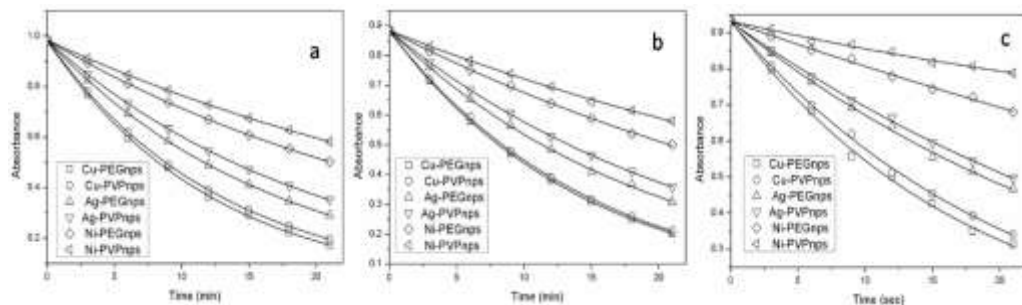


Fig. 7 - Absorbance vs Time plots for the M-nps catalyzed reductive degradation of three drugs a) Polybion b) Neurobion and c) Methycobal under Solar irradiation

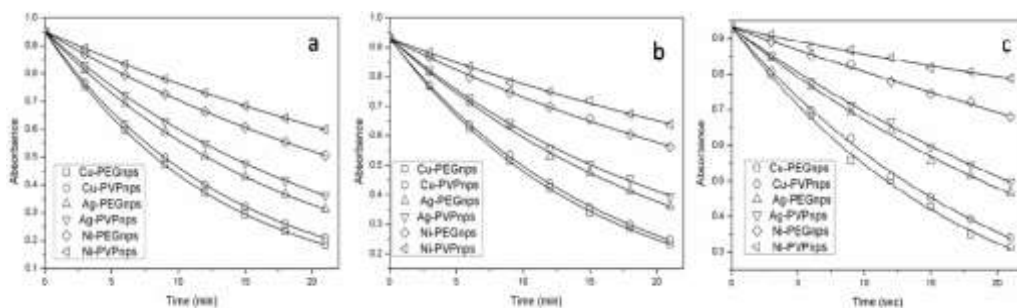


Fig. 8 - Absorbance vs Time plots for the M-nps catalyzed reductive degradation of three drugs a) Polybion b) Neurobion and c) Methycobal under UV irradiation

The rate coefficient values (k), catalytic efficiency (ϕ_c) and the half-life periods ($t_{50\%}$) determined for the degradation of drugs carried out under solar and UV irradiations in presence of PEG capped Cu-nps catalysts are presented in table 1. Analysis of rate coefficient of the catalysis (k values) carried out by Cu-PEG-nps inferred that the solar irradiation augmented drug degradation takes place at a better rate than that of the UV irradiation. The trend of catalytic efficiency (ϕ_c values) as recorded in the present study has been solar > UV irradiation. The higher influence of solar radiation could be attributed to its possession of high intensity natural UV rays and yellow light which facilitate faster catalysis of reductive degradation of drugs by M-nps [24].

Table 1 - Rate coefficient (k) values, times of 50% reduction and catalytic efficiency(ϕ_c) under pseudo first order conditions determined for the reduction of drugs using NaBH_4 and Cu-PEG-nps

Entry	Drugs	Solar irradiation			UV irradiation		
		k ($\times 10^{-4}$) s^{-1}	$t_{50\%}$ min	ϕ_c	k ($\times 10^{-4}$) s^{-1}	$t_{50\%}$ min	ϕ_c
1	PB	5.31	24	8.40	4.82	22	7.83
2	NB	4.12	31	7.85	3.80	20	5.50
3	MC	3.55	33	6.13	3.17	25	3.96

The kinetic plots of catalytic degradation of three drug systems under solar and UV irradiations by PEG and PVP stabilized M-nps are shown in figures 9 and 10. The linear relationship between the irradiation time and absorbance in terms of pseudo-first order kinetic of the photocatalytic degradation of drugs has been clearly recorded in the kinetic plots. It may be noted that the absorbance values (A/A_0) are on the decreasing trend with the length of the reaction time. It was found that after nearly for five catalytic cycles the rate coefficient values started to decrease indicating that the catalytic activity of the catalyst is decreasing. The

catalyst recovered after the fifth cycle when examined under FESEM and HRTEM photographs the particles are found agglomerated intensely. This effect causes a decrease in the catalytic activity, and thus, explains the observed results too. Similar study conducted on degradation of tetracycline using S-doped ZnO-nps by Farhadian et al. [26] explained that the linear correlation between the absorbance values with the reaction time is an index of pseudo first order for the reduction of dyes.

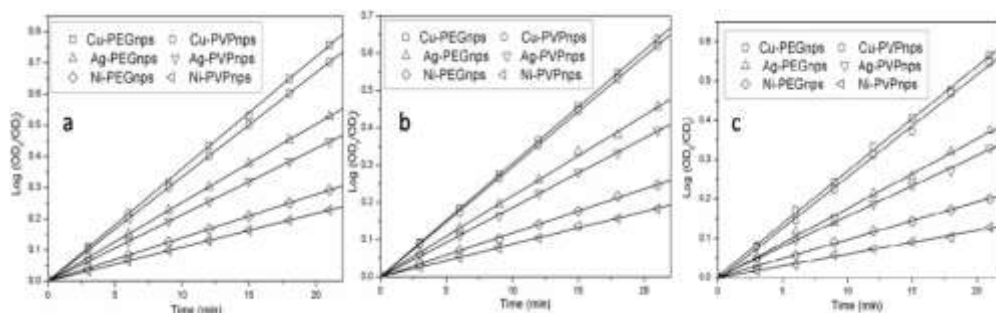


Fig. 9 - Kinetic for the M-nps catalyzed reductive degradation of three drugs a) Polybion b) Neurobion and c) Methycobal under Solar irradiation

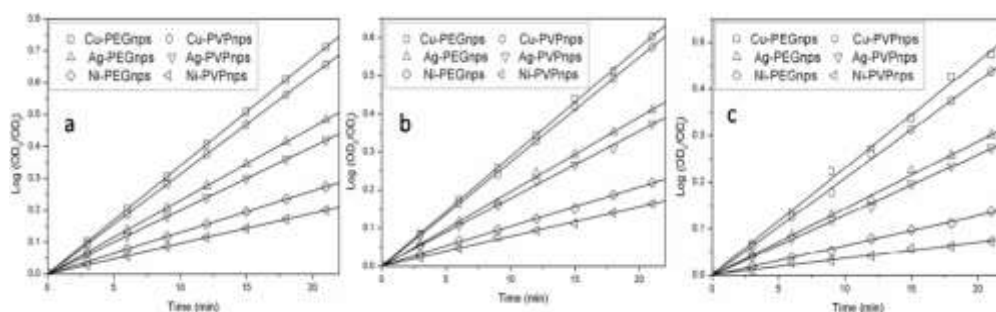


Fig. 10 - Kinetic for the M-nps catalyzed reductive degradation of three drugs a) Polybion b) Neurobion and c) Methycobal under UV irradiation

The table 2 represents the rate coefficient values of the degradation of the three drugs under UV and solar irradiations catalyzed independently by both PEG and PVP stabilized M-nps. Based on the observations of k -values of the reactions, the trend of catalytic efficiency of M-nps for the degradation of three drug systems was $\text{Cu} > \text{Ag} > \text{Ni}$ -nps. Further to the analysis catalytic potentials of M-nps of the present study indicated that the small sized Cu-nps exhibit higher rate coefficient than the large sized Ag-nps and Ni-nps. This could be due to the fact that the small sized nanoparticles possess large surface area to volume ratio and proportionate active sites which enable them to catalyze the reaction more efficiently. Apparently, the bio-stabilizer PEG results in the formation of smaller particles than the synthetic stabilizer, PVP. Keeping all the conditions constant, the trend of catalytic degradation of drugs with reference to the capping agents based on the recorded values was $\text{PEG} > \text{PVP}$. Research studies conducted elsewhere reported that the PEG has many hydroxyl (-OH) functional groups that aid the metal binding [27-29].

Table 2 - Rate coefficient k ($\times 10^{-4} \text{ s}^{-1}$) values under pseudo first order conditions determined for the reduction of drugs using NaBH_4 and Ag, Cu and Ni-nps with PEG, and PVP stabilizing agents

Dyes	SOLAR IRRADIATION						UV IRRADIATION					
	PEG			PVP			PEG			PVP		
	Ag nps	Cu nps	Ni nps	Ag nps	Cu nps	Ni nps	Ag nps	Cu nps	Ni nps	Ag nps	Cu nps	Ni nps
PB	4.07	5.80	3.92	4.62	5.14	3.42	3.86	4.83	3.13	4.75	4.85	2.98
NB	3.65	4.27	3.85	3.95	4.51	2.82	3.31	3.77	2.65	3.90	4.60	2.13
MC	3.12	3.45	2.66	3.44	3.96	2.17	3.14	3.52	1.97	3.32	3.93	1.87

The overall study of the mechanism of degradations of the drugs in the present study inferred that, the trend of photocatalytic degradation rate constants for the pharmaceutical drugs is in the order of $\text{MC} > \text{NB} > \text{PB}$. Our study has recorded that, owing to the compound constituted nature of the three drugs, the mean rate constant values for PB, NB and MC are similar to the degradation rate constant values of thiamine, nicotinamide and cyanocobalamine degradations respectively as reported from the studies of Bharathi et al. [30]. These observations underscores fact that the active ingredients of MC, NB and PB are cyanocobalamine, nicotinamide and thiamine. The comparatively efficient degradation of the drugs by the M-nps of the present study could be attributed to the target affinity based catalysis of active ingredients of these drugs.

CONCLUSION

Photocatalytic degradation of pharmaceutical drugs depends not only on the reaction time but also on the nature of the M-nps used. More efficient catalytic properties are associated with the cubic, smaller sized M-nps that are available in higher quantities. Catalytic reduction of drugs by M-nps takes place at an optimal temperature of 25°C and in the presence of the reducing agent NaBH_4 in the medium. Keeping all the conditions constant, with reference to pseudo-first order kinetic, the trend of degradation of the three drug systems is $\text{MC} > \text{NB} > \text{PB}$. The half-life periods ($t_{50\%}$) indicate that the catalytic activity of each M-nps catalyst system decrease after fifth or sixth catalysis cycle and the particles tend to agglomerate intensely. In terms of the catalytic efficiency (ϕ_c), the trend of degradation of the three drug systems by the M-nps is $\text{Cu} > \text{Ag} > \text{Ni-nps}$ and is inversely proportional to the size of M-nps ($\text{Cu} < \text{Ag} < \text{Ni nps}$). By virtue of facilitating smaller sized nanoparticles formation and tendering more $-\text{OH}$ groups, the PEG serves as a better stabilizing agent than PVP for M-nps mediated photocatalytic reactions. The natural solar irradiation, on account of possessing high intensity rays, can be a better candidate for facilitating reductive degradation of drugs than the sole UV radiation.

ACKNOWLEDGEMENTS

The authors thank the National center for Nanoscience and Nanotechnology, University of Madras for providing necessary facilities for performing characterization of metal nanoparticles synthesized in the present study.

DECLARATION

The authors declare that there are no conflicts of interest.

REFERENCES

1. Sharma, B. M., Bečanová, J., Scheringer, M., Sharma, A., Bharat, G. K., Whitehead, P. G., Klánová, J., & Nizzetto, L. (2019). Health and ecological risk assessment of emerging contaminants (pharmaceuticals, personal care products, and artificial sweeteners) in surface and groundwater (drinking water) in the Ganges River Basin, India. *Science of The Total Environment*, 646, 1459–1467. <https://doi.org/10.1016/j.scitotenv.2018.07.235>
2. Klammerth, N., Malato, S., Agüera, A., & Fernández-Alba, A. (2013). Photo-Fenton and modified photo-Fenton at neutral pH for the treatment of emerging contaminants in wastewater treatment plant effluents: A comparison. *Water Research*, 47(2), 833–840. <https://doi.org/10.1016/j.watres.2012.11.008>
3. Cheng, M., Zeng, G., Huang, D., Lai, C., Xu, P., Zhang, C., & Liu, Y. (2016). Hydroxyl radicals based advanced oxidation processes (AOPs) for remediation of soils contaminated with organic compounds: A review. *Chemical Engineering Journal*, 284, 582–598. <https://doi.org/10.1016/j.cej.2015.09.001>
4. Karthikeyan, K. G., & Meyer, M. T. (2006). Occurrence of antibiotics in wastewater treatment facilities in Wisconsin, USA. *Science of The Total Environment*, 361(1–3), 196–207. <https://doi.org/10.1016/j.scitotenv.2005.06.030>
5. Tang, W. Z., & Huren An. (1995). UV/TiO₂ photocatalytic oxidation of commercial dyes in aqueous solutions. *Chemosphere*, 31(9), 4157–4170. [https://doi.org/10.1016/0045-6535\(95\)80015-d](https://doi.org/10.1016/0045-6535(95)80015-d)
6. Ghosh, S. K., Kundu, S., Mandal, M., & Pal, T. (2002). Silver and Gold Nanocluster Catalyzed Reduction of Methylene Blue by Arsine in a Micellar Medium. *Langmuir*, 18(23), 8756–8760. <https://doi.org/10.1021/la0201974>
7. Ata, S., Shaheen, I., Qurat-ul-Ayne, Ghafoor, S., Sultan, M., Majid, F., Bibi, I., & Iqbal, M. (2018). Graphene and silver decorated ZnO composite synthesis, characterization and photocatalytic activity evaluation. *Diamond and Related Materials*, 90, 26–31. <https://doi.org/10.1016/j.diamond.2018.09.015>
8. Arshad, M., Abbas, M., Ehtisham-ul-Haque, S., Farrukh, M. A., Ali, A., Rizvi, H., Soomro, G. A., Ghaffar, A., Yameen, M., & Iqbal, M. (2019). Synthesis and characterization of SiO₂ doped Fe₂O₃ nanoparticles: Photocatalytic and antimicrobial activity evaluation. *Journal of Molecular Structure*, 1180, 244–250. <https://doi.org/10.1016/j.molstruc.2018.11.104>
9. Bhatia, V., & Dhir, A. (2016). Transition metal doped TiO₂ mediated photocatalytic degradation of anti-inflammatory drug under solar irradiations. *Journal of Environmental Chemical Engineering*, 4(1), 1267–1273. <https://doi.org/10.1016/j.jece.2016.01.032>
10. Chatzitakis, A., Berberidou, C., Paspaltsis, I., Kyriakou, G., Sklaviadis, T., & Poullos, I. (2008). Photocatalytic degradation and drug activity reduction of Chloramphenicol. *Water Research*, 42(1–2), 386–394. <https://doi.org/10.1016/j.watres.2007.07.030>

11. Chiang, L.-F., & Doong, R. (2014). Cu–TiO₂ nanorods with enhanced ultraviolet- and visible-light photoactivity for bisphenol A degradation. *Journal of Hazardous Materials*, 277, 84–92. <https://doi.org/10.1016/j.jhazmat.2014.01.047>
12. Dalrymple, O. K., Yeh, D. H., & Trotz, M. A. (2007). Removing pharmaceuticals and endocrine-disrupting compounds from wastewater by photocatalysis. *Journal of Chemical Technology & Biotechnology*, 82(2), 121–134. Portico. <https://doi.org/10.1002/jctb.1657>
13. Sun, Y., & Xia, Y. (2002). Shape-Controlled Synthesis of Gold and Silver Nanoparticles. *Science*, 298(5601), 2176–2179. <https://doi.org/10.1126/science.1077229>
14. Das, S. K., Khan, Md. M. R., Guha, A. K., Das, A. R., & Mandal, A. B. (2012). Silver-nano biohybride material: Synthesis, characterization and application in water purification. *Bioresource Technology*, 124, 495–499. <https://doi.org/10.1016/j.biortech.2012.08.071>
15. Muthukrishnan, S., Bhakya, S., Senthil Kumar, T., & Rao, M. V. (2015). Biosynthesis, characterization and antibacterial effect of plant-mediated silver nanoparticles using *Ceropegia thwaitesii* – An endemic species. *Industrial Crops and Products*, 63, 119–124. <https://doi.org/10.1016/j.indcrop.2014.10.022>
16. Hinojosa – Reyes, M., Camposeco – Solis, R., Ruiz, F., Rodríguez – González, V., & Moctezuma, E. (2019). Promotional effect of metal doping on nanostructured TiO₂ during the photocatalytic degradation of 4-chlorophenol and naproxen sodium as pollutants. *Materials Science in Semiconductor Processing*, 100, 130–139. <https://doi.org/10.1016/j.mssp.2019.04.050>
17. Mntungwa, N., Pullabhotla, V. S. R., & Revaprasadu, N. (2012). Facile Synthesis of Organically Capped CdTe Nanoparticles. *Journal of Nanoscience and Nanotechnology*, 12(3), 2640–2644. <https://doi.org/10.1166/jnn.2012.6133>
18. Basu, S., Maji, P., & Ganguly, J. (2015). Rapid green synthesis of silver nanoparticles by aqueous extract of seeds of *Nyctanthes arbor-tristis*. *Applied Nanoscience*, 6(1), 1–5. <https://doi.org/10.1007/s13204-015-0407-9>
19. Kaur, T., Sraw, A., Toor, A. P., & Wanchoo, R. K. (2016). Utilization of solar energy for the degradation of carbendazim and propiconazole by Fe doped TiO₂. *Solar Energy*, 125, 65–76. <https://doi.org/10.1016/j.solener.2015.12.001>
20. Krishnakumar, V., Boobas, S., Jayaprakash, J., Rajaboopathi, M., Han, B., & Louhi-Kultanen, M. (2016). Effect of Cu doping on TiO₂ nanoparticles and its photocatalytic activity under visible light. *Journal of Materials Science: Materials in Electronics*, 27(7), 7438–7447. <https://doi.org/10.1007/s10854-016-4720-1>
21. Malakootian, M., Olama, N., Malakootian, M., & Nasiri, A. (2018). Photocatalytic degradation of metronidazole from aquatic solution by TiO₂-doped Fe³⁺ nano-photocatalyst. *International Journal of Environmental Science and Technology*, 16(8), 4275–4284. <https://doi.org/10.1007/s13762-018-1836-2>
22. Ayodhya, D., & Veerabhadram, G. (2017). One-pot green synthesis, characterization, photocatalytic, sensing and antimicrobial studies of *Calotropis gigantea* leaf extract capped CdS NPs. *Materials Science and Engineering: B*, 225, 33–44. <https://doi.org/10.1016/j.mseb.2017.08.008>
23. Awfa, D., Ateia, M., Fujii, M., Johnson, M. S., & Yoshimura, C. (2018). Photodegradation of pharmaceuticals and personal care products in water treatment using carbonaceous-TiO₂ composites: A critical review of recent literature. *Water Research*, 142, 26–45. <https://doi.org/10.1016/j.watres.2018.05.036>
24. Shetty, R., Chavan, V. B., Kulkarni, P. S., Kulkarni, B. D., & Kamble, S. P. (2016). Photocatalytic Degradation of Pharmaceuticals Pollutants Using N-Doped TiO₂ Photocatalyst: Identification of CFX Degradation Intermediates. *Indian Chemical Engineer*, 59(3), 177–199. <https://doi.org/10.1080/00194506.2016.1150794>

25. Méndez, E., González-Fuentes, M. A., Rebollar-Perez, G., Méndez-Albores, A., & Torres, E. (2016). Emerging pollutant treatments in wastewater: Cases of antibiotics and hormones. *Journal of Environmental Science and Health, Part A*, 52(3), 235–253. <https://doi.org/10.1080/10934529.2016.1253391>
26. Farhadian, N., Akbarzadeh, R., Pirsaeheb, M., Jen, T.-C., Fakhri, Y., & Asadi, A. (2019). Chitosan modified N, S-doped TiO₂ and N, S-doped ZnO for visible light photocatalytic degradation of tetracycline. *International Journal of Biological Macromolecules*, 132, 360–373. <https://doi.org/10.1016/j.ijbiomac.2019.03.217>
27. Shi, W., Liu, C., Li, M., Lin, X., Guo, F., & Shi, J. (2020). Fabrication of ternary Ag₃PO₄/Co₃(PO₄)₂/g-C₃N₄ heterostructure with following Type II and Z-Scheme dual pathways for enhanced visible-light photocatalytic activity. *Journal of Hazardous Materials*, 389, 121907. <https://doi.org/10.1016/j.jhazmat.2019.121907>
28. Limpachanangkul, P., Jedsukontorn, T., Zhang, G., Liu, L., Hunsom, M., & Chalermssinsuwan, B. (2019). Comparative photocatalytic behavior of photocatalysts (TiO₂, SiC, Bi₂O₃, ZnO) for transformation of glycerol to value added compounds. *Korean Journal of Chemical Engineering*, 36(9), 1527–1535. <https://doi.org/10.1007/s11814-019-0326-7>
29. Wang, H., Yao, H., Pei, J., Liu, F., & Li, D. (2016). Photodegradation of tetracycline antibiotics in aqueous solution by UV/ZnO. *Desalination and Water Treatment*, 57(42), 19981–19987. <https://doi.org/10.1080/19443994.2015.1103309>
30. Bharathi, D., Ranjithkumar, R., Chandarshekar, B., & Bhuvaneshwari, V. (2019). Preparation of chitosan coated zinc oxide nanocomposite for enhanced antibacterial and photocatalytic activity: As a bionanocomposite. *International Journal of Biological Macromolecules*, 129, 989–996. <https://doi.org/10.1016/j.ijbiomac.2019.02.061>